TRENDS IN SCIENCES 2025; 22(7): 10129
https://doi.org/10.48048/tis.2025.10129 RESEARCH ARTICLE

The Potential of Chromatographic and Chemometric Profiling as Early Detection Tools for Metabolic Disturbances in Third-Hand Smoke-Exposed Rats: An Exploratory Study

Astari Pranindya-Sari[1], Reviono[1,3], Agus Dwi Susanto[2] and Dono Indarto[1,4,*]

[1]Doctoral Program of Medical Science, Faculty of Medicine, Universitas Sebelas Maret, Surakarta 57126, Indonesia
[2]Department of Pulmonology and Respiratory Medicine, Faculty of Medicine, Universitas Indonesia, Jakarta 10430, Indonesia
[3]Department of Pulmonology and Respiratory Medicine, Faculty of Medicine, Universitas Sebelas Maret, Surakarta 57126, Indonesia
[4]Biomedical Laboratory, Faculty of Medicine, Universitas Sebelas Maret, Surakarta 57126, Indonesia

([*]Corresponding author's Dono Indarto e-mail: dono@staff.uns.ac.id)

Received: 9 March 2025, Revised: 6 April 2025, Accepted: 13 April 2025, Published: 30 May 2025

Abstract

The application of chromatography in detecting toxicant-induced systemic alterations remains underexplored. Third-hand smoke (THS) exposure is increasingly recognised as a significant environmental health concern; however, its metabolic and haematological consequences are not yet fully characterised. This study investigates the potential of chromatographic profiling and chemometric analysis as tools for the early detection of metabolic disturbances induced by THS. Fifteen male Wistar rats were allocated to 3 groups: Control and THS exposure (12 or 24 cigarettes per day). Blood samples were collected at multiple time points for haematological analysis, while serum chromatography was conducted on day 10, and lung histology was assessed on day 30. Early metabolic disturbances were observed, characterised by the depletion of key amino acids (L-methionine, DL-lysine, DL-threonine, L-leucine, DL-arginine, and DL-carnitine) and elevated lipid biomarkers (palmitoyl sphingomyelin and phosphatidylcholine) in THS-exposed groups. These metabolic alterations preceded detectable haematological abnormalities. By day 30, haematological impairments and substantial pulmonary damage were evident. The depletion of essential amino acids and elevations in lipid biomarkers may serve as early indicators of toxicant-induced systemic effects. Chromatographic profiling detected metabolic perturbations prior to haematological and pulmonary impairments, highlighting its potential as an early toxicity detection tool. The findings of this exploratory study underscore the promise of chromatography for early toxicity detection, warranting further validation in larger cohorts.

Keywords: Chromatography, Third-hand smoke, Chemometric analysis, Metabolic biomarkers, Toxicant exposure, Early detection

Introduction

Despite its high sensitivity, chromatography remains underutilised in disease diagnostics, particularly within environmental toxicology. One emerging yet underexplored area where chromatography could prove invaluable is the study of THS exposure. THS refers to the residual tobacco pollutants that persist on indoor surfaces (e.g., dust, fabrics), posing prolonged health risks through dermal contact, ingestion, and inhalation [1]. Unlike the 1st- and 2nd-hand smoke (SHS), the insidious nature of THS has only recently garnered scientific attention. Studies indicate that THS contains over 250 harmful chemicals, many of which are implicated in carcinogenesis and systemic toxicity [2]. Growing evidence suggests that THS exposure induces oxidative stress, inflammation-

particularly pyroptosis- and cellular dysfunction, ultimately leading to progressive organ damage [3]. Identifying early metabolic alterations associated with THS toxicity remains a significant challenge. In this study, we hypothesise that chromatographic profiling, combined with chemometric analysis, could serve as a sensitive approach for detecting early metabolic disruptions induced by THS exposure, preceding the onset of haematological abnormalities and pulmonary damage (e.g., damage underpinned by pyroptosis, as indicated by IL-18). Through this analytical framework, we aim to evaluate its potential in identifying biochemical alterations in Wistar rats exposed to THS, thereby providing novel insights into the early metabolic consequences of prolonged exposure.

Materials and methods

Cigarette and smoking apparatus

Commercial unfiltered cigarettes containing 2.5 mg nicotine per cigarette, as indicated on the packaging, were used in this study. Tobacco smoke, simulating active smoking, was generated using an apparatus equipped with a 3.6 kPa vacuum suction system. This device mimicked smoking behaviour by alternating between a 3-second inhalation- (ON) and a 4-second rest-phase (OFF) in a continuous cycle (**Figure 1**).

Solution for chromatography

Chromatographic analysis was performed on cage rinsates using Liquid Chromatography-Mass Spectrometry (LCMS)-grade methanol (MeOH) from Fisher Scientific (USA). Calibrant solution from the Pierce LTQ Velos, ESI negative and positive ion calibration solution (Thermo Scientific, Rockford, IL, USA). The samples were stored in 30 mL dark amber tubes, sealed with screw caps, and secured with polytetrafluoroethylene (PTFE) tape. Additional materials required for the procedure included Eppendorf tubes, sterile syringes, and sterile gauze.

Urine cotinine and lung interleukin (IL)-18 measurements

Mouse/rat Cotinine Enzyme-Linked Immunosorbent Assay (ELISA) kit was procured from Calbiotech® (CA, USA), and for IL-18 was supplied by Elabscience® (China).

The THS-cage

The primary objective of this stage was to establish a "THS environment" within the rat cages as their living space, providing evidence of tobacco smoke residue on the interior surfaces, even after the smoke was no longer visible. Three transparent plastic cages (484×322×262 mm^3) with airtight, well-fitted lids and minimal ventilation were allocated to 3 groups: A control cage (exposed to clean air), a THS-A cage (exposed to 12 cigarettes per day for 5 days), and a THS-B cage (exposed to 24 cigarettes per day for 5 days). The THS cages were converted into THS exposure environments by introducing cigarette smoke generated by a custom-built smoking apparatus (**Figure 1**) under controlled temperature conditions (24 - 25 °C) with no direct sunlight. The plastic material facilitated the retention of smoke within the enclosed space, minimising leakage and ensuring consistent exposure levels. Additionally, a blower was employed during exposure to ensure the uniform distribution of cigarette smoke, maximising contact with all interior surfaces.

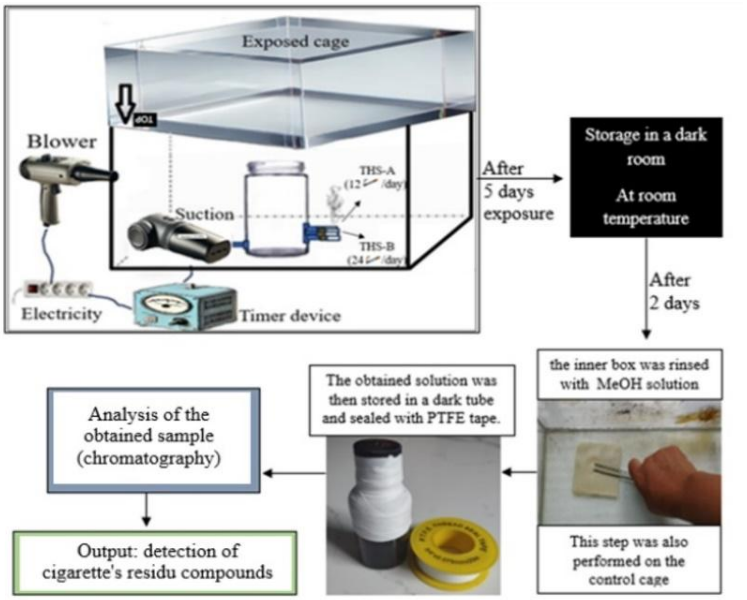

Figure 1 Experimental setup for THS exposure and residue analysis. The schematic illustrates the procedure for establishing a THS-exposed environment and analysing cigarette residue compounds. The cages were placed upside down to maximise exposure to cigarette smoke.

The cages were stored in a dark room for 2 days following each 5-day exposure cycle to allow THS residue deposition. Subsequently, the inner surfaces of all cages (including the control) were rinsed with approximately 30 mL of methanol (MeOH). Methanol was selected due to its high efficiency in dissolving substances [4], previously used for nicotine extraction [5] and has been considered an "entrainer" compound [6] based on past studies, ensuring the effective extraction of THS residues from the cage surfaces. This step was essential to obtain accurate and reproducible chemical profiles of THS deposits, ensuring the effective extraction of target substances and minimising the risk of false-negative results due to incomplete recovery during the swabbing process. The extracted residues were collected in amber tubes and sealed with PTFE tape to prevent evaporation or contamination before analysis. A qualitative assessment of the residues was conducted using Ultra-Performance Liquid Chromatography-High-Resolution Mass Spectrometry (UHPLC-HRMS). The treatment series was repeated 3 times to ensure data reproducibility.

The cages rinsed with MeOH were not reused for any subsequent steps, particularly for housing the rats, in order to prevent any potential residual MeOH from entering the rats' bodies. This was a necessary precaution, as MeOH was not the compound being studied, and we aimed to avoid any unintended exposure to it. The use of MeOH for rinsing was solely intended for the purpose of verifying and optimizing the cages for tobacco residue presence. Once the GCMS analysis confirmed the presence of tobacco residue on the cages, this marked the successful completion of the cage optimization phase. At that point, the process was deemed complete, and the outcome became the standard operating procedure (SOP) for creating the THS-contaminated cages in this study. Subsequently, new cages were prepared according to the SOP, ensuring they were appropriately exposed to THS. These newly prepared cages were then used to house the rats. This procedure ensures that only cages containing the desired tobacco residue are used for animal housing, and no residual MeOH contaminates the exposure environment.

The Third-Hand Smoker rat model

The primary objective of this stage is to confirm that tobacco smoke residue adhering to the interior surfaces of the cage is indeed transferred into the rats' bodies, providing sufficient justification to classify the exposed rats as "Third-Hand Smoker rats". Fifteen male Wistar rats (n = 5 per group) were randomly placed to 3 groups: Control, THS-A, and THS-B cage. Rats experienced adaptation for 1 week prior to the randomisation with ad libitum access to food (Ratbio®)

and water. Rats in THS cages were classified as "Third-Hand Smoker rats" based on the detection of cigarette residues in their urine using UHPLC-HRMS, compared to the rats in control cage. The total duration of rat exposure in each cage, according to their respective groups, was 30 days. The cages were replaced weekly, following the appropriate treatment for each group. All experimental procedures involving animals adhered to institutional and international ethical standards and were approved by the Institutional Animal Care and Use Committee, Faculty of Medicine, Universitas Sebelas Maret, Surakarta, Indonesia, under Ethical Clearance Number 112/UN27.06.11/KEP/EC/2024.

Urine and blood sampling

Urine samples were obtained on day 10 of exposure. A 24-hour urine collection was conducted for each rat using a metabolic cage, with samples collected in sterile tubes and stored at −20 °C for analysis. From the retro-orbital sinus, the blood was collected. Two types of blood analyses were planned: Blood tests and serum analysis. For routine blood test using an automated blood analyser, 0.5 mL of blood was collected into Vacutainer EDTA tubes at several time points: Baseline (day 0), day 10, and day 30. At the start of the study, blood cell components which was previously reported to be affected by cigarette exposure based on literature [7] were assessed to ensure no significant baseline differences among groups (the baseline/day 0). For serum analysis, the day 10 and day 30 blood samples were collected into 1.5 mL microtubes and centrifuged at 3,000 rpm (10 min). The supernatant was carefully transferred into a new, pre-sterilised 1.5 mL microtube and stored at −20 °C until further analysis. To further explore the progression of haematological alterations over time, an additional assessment was conducted on day 20 as an intermediate measurement provided supplementary insights into potential progressive trends between the predefined time points, offering a more comprehensive representation of haematological changes throughout the exposure period.

Chromatography and chemometric analysis

Extraction was carried out to day-10 serum and urine samples following the established protocol [8], with modifications in the ionisation mode. Two-millilitre microcentrifuge tubes were prepared, filled with either 50 µL serum or 100 µL urine. Sample extraction was carried out using 1 mL of LCMS grade MeOH (to serum) and water (to urine) ensuring optimal analyte solubility. Vortexed for 60 s to facilitate homogenisation, followed by sonication at room temperature for 30 min to enhance metabolite extraction. Separation phase was achieved by centrifugation at 3,000 rpm, after which the supernatant was carefully collected and filtered through a 0.22 µm nylon syringe filter to remove particulates. LCMS grade MeOH and water were occupied as blank samples to minimise background interference.

Liquid chromatography analysis was conducted using a Thermo Scientific™ Accucore™ C-18 analytical column (100×2.1 mm ID, 2.6 µm). A gradient elution method was employed, utilizing LCMS-grade water (solvent A) and methanol (solvent B), both containing 0.1 % formic acid, with a flow rate maintained at 300 µL/min. The mobile phase composition initially consisted of 95 % solvent A, which was gradually decreased to 5 % over a 16-minute duration. This composition was held at 5 % for 4 min before returning to the starting condition (95 % solvent B) over the next 25 min.

For untargeted screening, both positive and negative ionization modes were applied in full MS/dd-MS2 acquisition mode. Nitrogen was used as the auxiliary, sweep, and sheath gas, with respective settings of 32, 8, and 4 arbitrary units (AU). The instrument settings included a spray voltage of 3.30 kV, a capillary temperature of 320 °C, and an auxiliary gas heater temperature of 30 °C. The scan range was set between 66.7 - 1,000 m/z, with a resolution of 70,000 for full MS and 17,500 for dd-MS2 analysis. The system was operated using XCalibur 4.4 software (Thermo Scientific, Bremen, Germany). Instrument performance was optimized through calibration with Thermo Scientific Pierce ESI ion calibration solutions before analysis, ensuring accuracy in ion transfer, detection, and sensitivity.

Metabolite profiling of control, THS-A, and THS-B groups was conducted using an untargeted metabolomics approach with Thermo Scientific's Compound Discoverer® software. MS2 filtering was applied to isolate the target ions, and the results—including blank samples (methanol and water)—were analyzed using the MzCloud database for compound

identification. Chemometric analysis was performed using Partial Least Squares Discriminant Analysis (PLS-DA) to differentiate treatment groups from controls. The statistical analysis was conducted using MetaboAnalyst 6.0, incorporating the identified chemical and metabolite features as classification variables.

Lung tissue preparations

Intraperitoneal injection of an anaesthetic (euthanasia) mixture containing Xylazine 7.5 mg/kg, Ketamine 60 mg/kg, and Acepromazine 2 mg/kg. The lungs were dissected for further analysis. The collected organs were processed as follows: 1) The left lung was fixed in 10 % neutral buffered formalin (NBF) and maintained at room temperature for histopathological examination; 2) The right lung lobes were immediately placed in 1.5 mL microtubes and stored at −80 °C for enzyme-linked immunosorbent assay (ELISA). For histopathological analysis, the right lung lobe was selected based on established anatomical and methodological considerations. In rodents, the right lung is larger and structurally distinct from the left. Previous studies have employed a similar approach to ensure consistency and reproducibility in comparative analyses [9,10].

Measurement of urinary cotinine and lung IL-18

Urinary cotinine and lung IL-18 levels were quantified using ELISA in accordance with the reagent manufacturer's protocol. The reagent protocols are included in the supplementary material.

Hematoxylin and Eosin (HE) Staining

For histopathological analysis, the left lung lobe of each rat was meticulously excised and fixed in 10 % neutral buffered formalin (NBF). After fixation, the tissue samples were embedded in paraffin blocks, sectioned into 5-µm-thick slices, and stained with HE. Histological assessment was performed using a light microscope at ×10 and ×40 magnifications.

Statistical analysis

All data were analysed using SPSS Statistics for Windows, licensed Version 26.0 (IBM Corp., Armonk, NY, USA) and are presented as mean ± standard deviation (SD). Data normality was assessed using the Shapiro-Wilk test, and statistical analysis was performed accordingly. For normally distributed data, one-way analysis of variance (ANOVA) was used to compare urine cotinine, lung IL-18 levels, haematological parameters, and to assess significant differences in the chemometric data across experimental groups. Kruskal-Wallis test was applied for non-normally distributed data. A $p < 0.05$ was considered statistically significant.

Results and discussion

THS cage as a THS environment for experimental rats

The GCMS analysis detected the presence of nicotine and other cigarette-derived residues in the MeOH-extracted liquid obtained from swabbing and rinsing the inner surfaces of the exposed cages. In contrast, no nicotine or cigarette residue was detected in the control group (**Figure 2**). The THS-A sample demonstrated the presence of nicotine, β-guaiene, and 1,2-benzenedicarboxylic acid, compounds commonly associated with tobacco smoke residues. The THS-B sample exhibited benzene, eugenol, and 1,2-benzenedicarboxylic acid. Benzene and eugenol were more prominent in THS-B, suggesting variability in compound deposition and retention across different THS exposure conditions. The detection of 1,2-benzenedicarboxylic acid in both THS-A and THS-B samples indicates that certain cigarette-derived pollutants persisted across different exposure scenarios. The control sample displayed no significant compounds, reinforcing the notion that THS exposure resulted in the accumulation of tobacco-specific residues within the experimental environment.

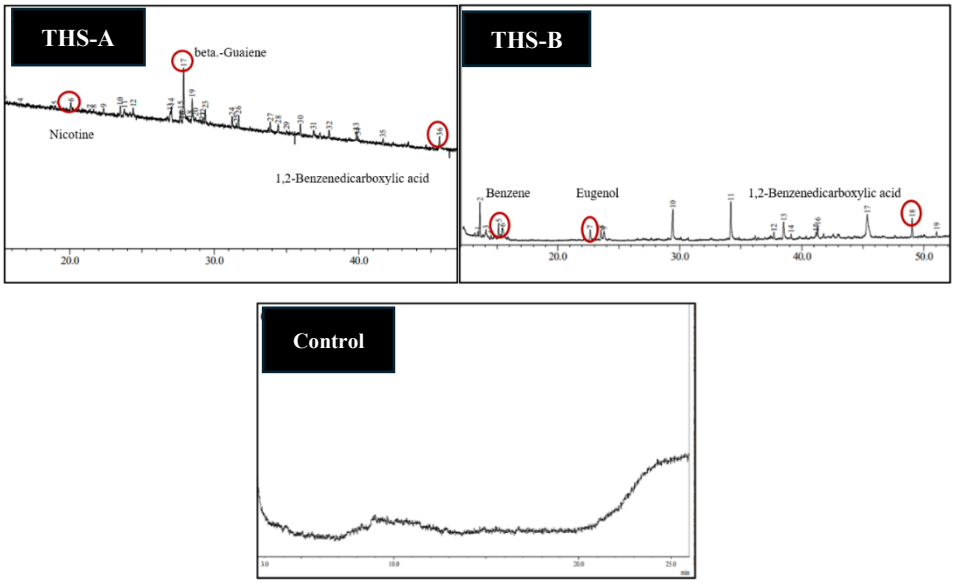

Figure 2 Gas chromatography-mass spectrometry (GC-MS) analysis of THS and control samples. THS-A sample showing the presence of nicotine, β-Guaiene, and 1,2-benzenedicarboxylic acid. THS-B sample displaying benzene, eugenol, and 1,2-benzenedicarboxylic acid. Control sample showing no significant volatile organic compounds detected. Identified peaks are marked with red circles.

Data from cage analysis confirm that the THS-A and THS-B cages met the 'residual' criterion of THS, establishing them as THS-exposed environments. Notably, the absence of cigarette-related compounds in control samples strengthens the reliability of the GCMS findings, confirming that the identified compounds originated specifically from THS residues. These results align with previous studies on THS exposure and its biological impact [2,11]. With the presence of cigarette residues in the cage environment confirmed, the study proceeded to investigate the effects on rats that were housed within these conditions.

Third-Hand Smoker rat model evidenced by detection of cigarette residues in the urine

Following the confirmation of cigarette-residue compounds in the exposed cages, further investigations were conducted to determine the transfer of these substances to rats inhabiting the THS environment. Rats exhibit metabolic and physiological similarities to humans [12,13] making them a valuable model for predicting early biochemical markers of toxicity. Furthermore, their controlled experimental environment allows for precise exposure assessment, minimising the confounding variables often encountered in human studies. In addition to these reasons, conducting this study directly on humans would raise significant ethical concerns, particularly since "Third-Hand smoker" may not necessarily be individuals suffering from illnesses that would warrant invasive diagnostic procedures, such as lung biopsies. Therefore, an experimental animal model is crucial for advancing research in this field.

Table 1 Detected cigarette residues in the urine of THS-exposed rats compared to control rats.

Compound	Chromatography analysis			
	Cigarette	Day 10-urine samples of:		
		Control	THS-A	THS-B
4-Ethoxy-m-anisaldehyde	+	–	+	+
7-hydroxy-6-methoxy-2H-chromen-2-one	+	–	+	–
3-Amino-5-hydroxybenzoic acid	+	–	+	–

Compound	Chromatography analysis			
	Cigarette	Day 10-urine samples of:		
		Control	THS-A	THS-B
3-Hydroxy-2-methylpyridine	+	–	+	+
4’-Methoxyacetophenone	+	–	+	–
Eugenol	+	–	+	+
Eugenol Sulfate	+	–	+	+
trans-Anethole	+	–	+	+
Undecanedioic acid	+	–	+	+
Scopoletin	+	–	+	+
Hispidulin	+	–	–	+
Cotinine	Nicotine	–	+	+

The selection of a 30-day exposure duration represents a novel aspect of this study, as no standardised guideline currently exists THS exposure in rodent models. Historically, study investigating the effects of THS have primarily employed prolonged exposure durations, such as 196 days [2]. More recently, however, shorter exposure periods have been adopted, for instance investigated platelet responses following 3 months of THS exposure [14], and implemented a 3-week exposure period [7], although their outcome assessments were conducted several weeks post-exposure. Additionally, while not specifically focused on THS, Ho *et al*. [15] examined the effects of cigarette smoke (CS) exposure—which more closely represents SHS—over 4 weeks in a mouse model of experimental autoimmune encephalomyelitis.

Informed by these findings, we selected a 4-week exposure period to investigate whether metabolic and pulmonary alterations could be detected within this timeframe—an area that has yet to be explored in the context of THS exposure. This duration allows for the assessment of both early and later-stage effects while ensuring methodological feasibility and alignment with emerging toxicological research trends. Furthermore, it remains plausible that certain pathological effects identified after 3 months of exposure may already be present within the 1st month. By capturing this earlier stage, our study aims to provide a more comprehensive understanding of the onset and progression of THS-induced alterations.

Gas chromatography-mass spectrometry analysis of urine samples collected on day 10 from exposed and control rats revealed the presence of cigarette-derived residues exclusively in the THS-exposed group. These findings provide robust evidence that rats housed in a THS environment undergo sustained exposure, validating this model for studying THS-related toxicity. The confirmed chromatographic profiling of cotinine in urine samples qualitatively (**Table 1**) was further analyzed to determine the extent of cotinine accumulation in each group. The results revealed a significant increase in urinary cotinine levels in the THS-exposed groups (**Figure 3**). Consistent with the presence of THS residues in the cage environment, the detection of cigarette residues in urine indicates systemic absorption and metabolic processing of THS compounds in exposed rats [16-18]. The elevated urinary cotinine levels further confirm significant absorption of nicotine following THS exposure, reinforcing the potential of biomarker-based assessments for evaluating THS-related toxicokinetic. Beyond nicotine metabolism, the exposure appears to disrupt fundamental biochemical pathways, including amino acid homeostasis, which is critical for erythropoiesis and immune function.

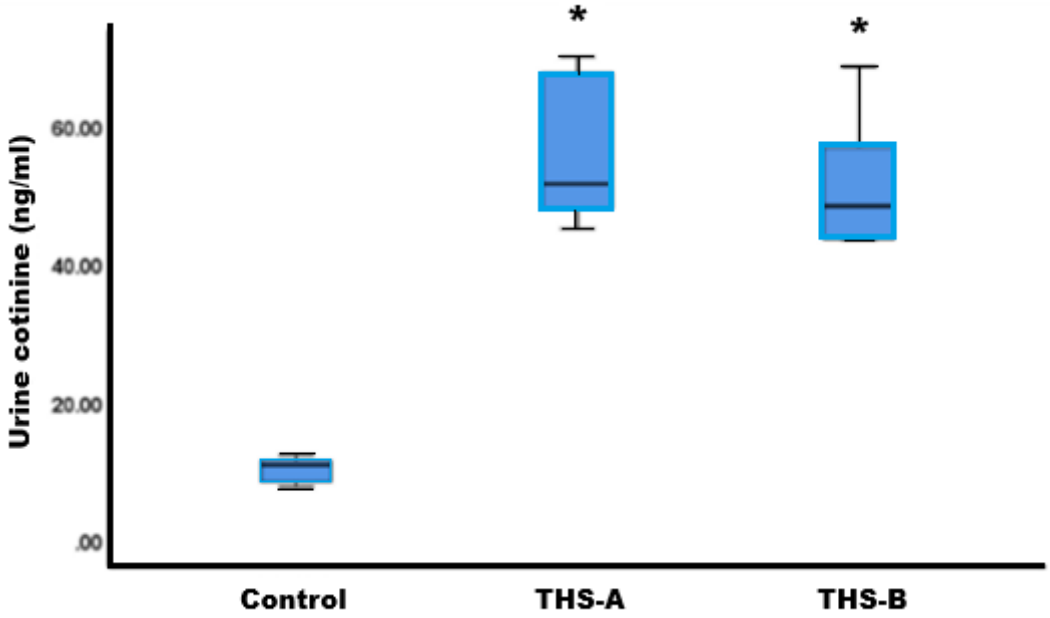

Figure 3 Urine cotinine levels (ng/mL) in control and THS-exposed groups (mean ± SD). Asterisks (*) denote statistically significant differences ($p < 0.05$) compared to the control group. The mean cotinine levels were 10.02 ± 1.9 ng/mL for the control group, 52.32 ± 9.61 ng/mL for THS-A, and 48.62 ± 16.28 ng/mL for THS-B. The data followed a normal distribution (Shapiro-Wilk test, $p > 0.05$ for all groups) with homogeneity of variance confirmed by Levene's test ($p > 0.05$). Therefore, statistical analysis was conducted using ANOVA followed by Bonferroni post-hoc. No significant difference was observed between the THS-A and THS-B groups.

Early metabolic disruptions before haematological alterations: Role of chemometric analysis with chromatography

A reduction in L-methionine, DL-lysine, DL-threonine, L-leucine, DL-arginine, and DL-carnitine levels was observed in THS-exposed groups on day 10 compared to controls. L-methionine and DL-threonine, both essential for erythropoiesis and iron metabolism, exhibited notable declines, alongside L-leucine, which plays a role in haematopoietic function. It was only by day 30 that progressive haematological alterations became evident, including reductions in haemoglobin levels, erythrocyte count, and lymphocyte percentage in THS-exposed groups.

The depletion of amino acids essential for immune function and haematopoiesis corresponded with a decline in immune cell turnover, as evidenced by decreased lymphocyte counts in THS-exposed rats by day 30. The observed alterations in red blood cell parameters and immune profiles indicate progressive haematological changes following THS exposure. These findings demonstrate early metabolic disturbances in amino acid homeostasis preceding the onset of haematological impairments.

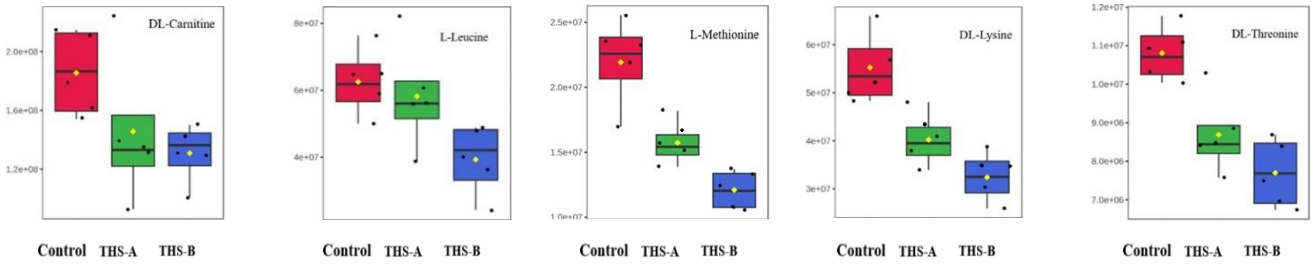

(a)

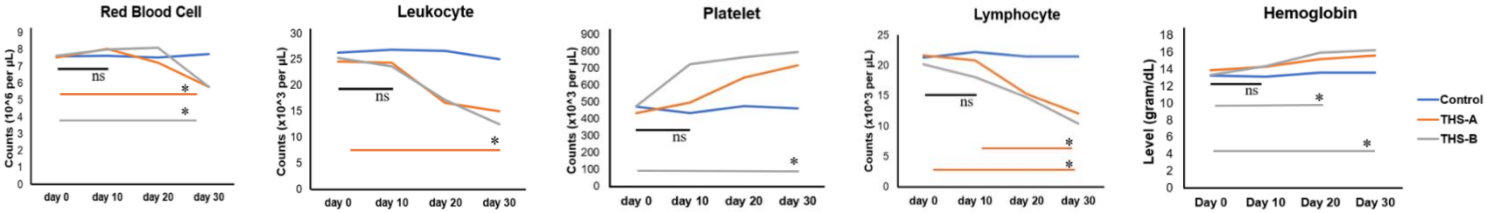

(b)

Figure 4 (a) Box plots showing the day10 blood samples with alterations in amino acid levels (Lmethionine, DL-lysine, DL-threonine, L-leucine, DL-arginine, and DL- carnitine). Despite no observable changes in routine blood examination at this stage, chromatographic analysis detected metabolic disturbances in THS-exposed groups compared to control. (b) Line graphs depicting haematological parameter changes over time (Days 0, 10, 20, and 30) in Control, THS-A (12 cigarettes/day exposure), and THS-B (24 cigarettes per day exposure) groups. Pathological alterations, including anemia, only became evident through routine blood analysis on day 30. * = Statistical significance ($p < 0.05$); ns = not-significant.

L-methionine and DL-threonine play crucial roles in erythropoiesis and iron metabolism, with evidence suggesting that their supplementation enhances haemoglobin levels and facilitates iron absorption [19]. L-methionine also serves as a key precursor for glutathione synthesis, crucial for redox balance and erythropoiesis [20]. Similarly, DL-lysine contributes to haemoglobin synthesis and erythrocyte integrity [19] while L-leucine has been shown to ameliorate anaemia in transfusion-dependent patients and regulate protein synthesis and immune cell proliferation [21]. DL-arginine plays a pivotal role in nitric oxide production, influencing vascular function and immune responses and it is essential for mitochondrial fatty acid metabolism, supports energy production in rapidly dividing cells, including erythroid and immune cells [22]. The depletion of these amino acids may have contributed to impaired erythropoiesis, reduced immune cell turnover, and heightened vulnerability to subsequent haematological impairments, as observed by day 30. These findings suggest that early metabolic disruptions in amino acid homeostasis may serve as predictive markers of impending haematological decline.

Chromatography analysis reveals early phosphatidylcholine and palmitoyl sphingomyelin alterations linked to IL-18-mediated pyroptosis and subsequent lung damage due to THS exposure

Chromatographic analysis of blood samples collected on day 10 of THS exposure revealed alterations in phosphatidylcholine ($p < 0.05$) and palmitoyl sphingomyelin, which varied according to the exposure group. Despite the absence of detectable haematological abnormalities at this stage (**Figure 4(b)**) and the inability to assess lung damage at this time point (as the time for rat sacrifice had not yet arrived), the metabolic changes observed suggest an early disruption in lipid homeostasis, which may serve as a precursor to later pathological changes.

Beyond amino acid metabolism, lipid homeostasis also plays a fundamental role in maintaining cellular integrity and regulating inflammatory signalling, making it a key factor in toxicant-induced damage. This study further highlights early disruptions in sphingomyelin and significant changes in phosphatidylcholine metabolism following THS exposure, suggesting a mechanistic link to inflammasome activation, pyroptosis, and pulmonary injury. Sphingomyelins, including palmitoyl

sphingomyelin, are essential for membrane stability and lipid signalling, particularly in inflammatory and apoptotic pathways [23,24]. The alterations in palmitoyl sphingomyelin levels observed in THS-exposed rats may indicate early ceramide accumulation, a well-documented trigger of NLRP3 inflammasome activation and pyroptotic cell death [25]. Ceramide accumulation has been linked to gasdermin D (GSDMD) cleavage [26], a hallmark of pyroptosis, suggesting that THS exposure may initiate a cascade of lipid-mediated inflammasome activation, leading to subsequent pulmonary damage. Pyroptotic cell death, characterised by membrane pore formation and IL-18 release, could contribute to the progressive inflammatory response seen in THS-exposed lungs. Although lung histopathology could not be assessed on day 10 because the rats had not yet been sacrificed, the early metabolic shifts detected via chromatography suggest a potential link to pyroptotic mechanisms, which may have contributed to the lung injury observed on day 30.

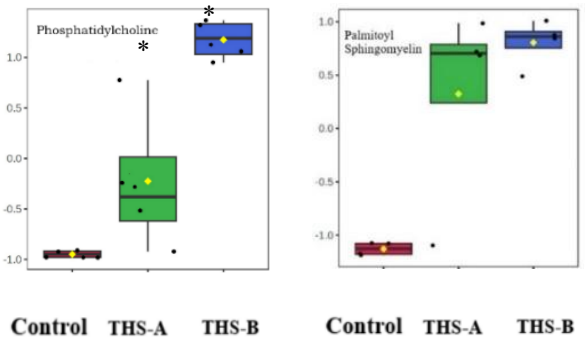

(a) Chemometrics result (day 10 blood samples)

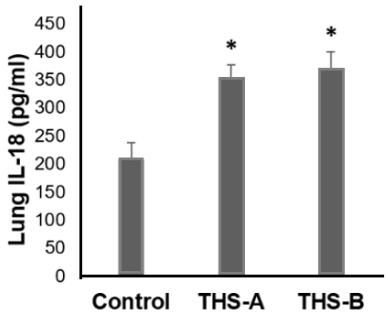

(b) ELISA IL-18 (day 30 lung samples)

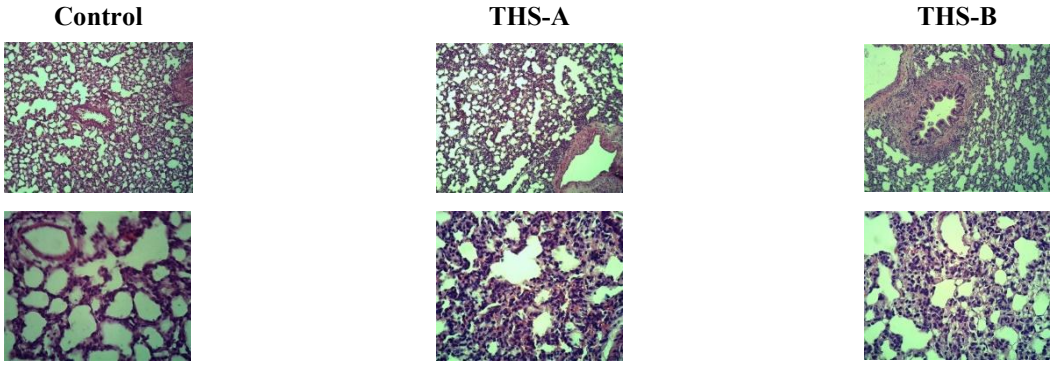

(c) Histological HE staining (day 30 lung samples)

Figure 5 Chromatographic and histopathological analysis of THS exposure in Wistar rats: (a) Chromatographic-approaches of day 10 blood samples revealed significant alterations in phosphatidylcholine and palmitoyl sphingomyelin levels across exposure groups. THS-A and THS-B groups exhibited exposure-dependent changes, suggesting early metabolic disturbances before the onset of detectable haematological abnormalities. (b) Lung IL-18 levels measured in day 30 lung samples showed a significant increase in THS-exposed groups compared to controls, indicating inflammasome activation and pyroptotic response. (c) Representative histological images of lung tissues (H&E staining, day 30) demonstrate progressive structural damage in THS-A and THS-B groups compared to the control, including alveolar thickening, inflammatory infiltration, and airway remodelling. These findings suggest a correlation between early lipidomic alterations, pyroptosis-driven inflammation, and subsequent lung damage. Statistical significance (*) ANOVA $p < 0.05$.

The delayed but significant elevation of IL-18 levels in THS-exposed groups further supports the hypothesis that lipid metabolism dysregulation precedes inflammasome activation and inflammatory lung injury (209.52 ± 33.52, 352.8 ± 27.4, and 363.4 ± 30.4 represented Control, THS-A and THS-B group,

respectively). Analysis of variance (ANOVA) revealed a statistically significant difference ($p < 0.05$), with Bonferroni post-hoc analysis indicating significant differences between the Control group and both THS-A and THS-B. Given the established role of IL-18 in inflammasome-driven pathology, these findings reinforce the importance of lipidomic disturbances as early indicators of lung inflammation and pyroptotic progression. Notably, chromatography-based lipid profiling enabled the detection of metabolic perturbations well before overt histopathological or clinical manifestations emerged, underscoring its potential for early-stage toxicological assessments and intervention strategies targeting pyroptosis-related pathways.

Disruptions in other key, the phospholipid pathways, may further contribute to THS-induced toxicity. Among these, phosphatidylcholine (PC) plays a central role in maintaining membrane integrity, lipid metabolism, and inflammatory regulation [27]. In environmental toxicology, exposure to hazardous compounds—which may well include THS—has been associated with disruptions in phospholipid homeostasis, potentially leading to cellular dysfunction even before overt pathological changes become evident [28]. This aligns with previous findings that aberrant phosphatidylcholine metabolism may serve as a preclinical biomarker in both human and animal studies [29-31]. In parallel with palmitoyl sphingomyelin dysregulation, one of the key pathways through which phosphatidylcholine disturbances contribute to disease progression is NLRP3 inflammasome activation [32,33]. The breakdown products of phosphatidylcholine, particularly lysophosphatidylcholine (LPC) and ceramides, have been implicated in pyroptotic signalling [34]. In the context of THS exposure, early phosphatidylcholine dysregulation may precede IL-18 elevation, marking the onset of chronic inflammation and progressive lung damage.

This study highlights the pivotal role of chromatographic profiling as a highly sensitive analytical tool for detecting early metabolic disturbances preceding haematological and pulmonary impairments induced by THS exposure. The observed depletion of key amino acids and disruptions in palmitoyl sphingomyelin as well as significant change in phosphatidylcholine metabolism suggest that metabolic alterations may serve as preclinical biomarkers of toxicant-induced systemic damage. The absence of haematological abnormalities on day 10 does not exclude underlying biochemical disruptions but rather underscores the limitations of conventional blood tests in detecting subtle metabolic shifts.

The early depletion of key amino acids was subsequently followed by alterations in haematological profiles. In this study, THS exposure served as a representative example of a hazardous environmental stimulus capable of inducing pathological conditions. The presence of this “hidden danger” at an early stage appears to have been detected through chromatography before conventional blood tests revealed any abnormalities. For instance, anaemia and thrombocytosis only became apparent on day 30. This delay is likely attributable to the fact that inflammatory responses may require distinct timeframes to manifest subsequent pathological effects. The observed increase in platelet levels on day 10 may be attributed to an inflammatory response triggered by THS. This phenomenon is likely mediated by pro-inflammatory cytokines such as interleukin-6 (IL-6), which plays a crucial role in megakaryopoiesis and platelet production. Several studies have demonstrated the correlation between acute inflammatory cytokines and thrombocytosis. For instance, Zhang *et al*. reported that elevated IL-6 levels induce thrombocytosis through enhanced cGMP-dependent protein kinase I signalling [35], also result on IL-6 has been shown to upregulate thrombopoietin (TPO) expression, thereby promoting platelet proliferation and activation as a compensatory response to vascular injury and systemic inflammation [36]. Conversely, the anaemia-related changes observed on day 30 likely represent a more progressive pathological outcome of prolonged THS exposure. Chronic oxidative stress, systemic inflammation, and potential bone marrow suppression could contribute to erythrocyte depletion and impaired haematopoiesis, ultimately leading to the observed reduction in red blood cell parameters at a later stage. The delayed onset of anaemia suggests that early metabolic disturbances and oxidative damage precede overt haematological alterations, reinforcing the importance of identifying these subclinical changes at an early stage [37,38].

From a translational perspective, these findings highlight the necessity of incorporating chromatography

into biomonitoring and early diagnostic frameworks, particularly for populations at heightened risk of chronic toxicant exposure, including passive smokers, industrial workers, and individuals with pre-existing respiratory conditions. Detecting metabolic alterations before haematological abnormalities manifest presents a critical opportunity for pre-emptive interventions, such as dietary or pharmacological modulation of amino acid homeostasis to prevent systemic damage. The use of THS as an exposure model exemplifies a broader category of 'hidden' environmental hazards—chronic yet imperceptible toxicant exposures that induce physiological disturbances long before clinical symptoms arise. Many environmental pollutants, including airborne contaminants, persistent organic chemicals, and indoor toxicants, share this characteristic. This approach could extend to other environmental toxicants, aiding in the development of predictive biomarkers for exposure-related diseases. By advancing highly sensitive analytical methodologies such as chromatography, future research may drive a paradigm shift towards proactive environmental health monitoring, enabling timely interventions and reducing the long-term burden of exposure-related diseases.

This study presents a novel approach to the early detection of metabolic disturbances induced by THS exposure through the integration of chromatographic profiling and chemometric analysis. The results emphasise the need to integrate advanced analytical techniques with routine haematological assessments to improve the early detection of toxicant exposure-related pathophysiology. While previous research on THS toxicity has predominantly relied on histopathological and haematological assessments, this study's findings demonstrate that metabolic alterations occur prior to overt systemic damage. This underscores the potential of chromatographic techniques as a sensitive tool for detecting early biochemical disruptions in response to environmental toxicants. A key strength of this study lies in the identification of specific metabolic perturbations, notably the depletion of essential amino acids (L-methionine, DL-lysine, DL-threonine, L-leucine, DL-arginine, and DL-carnitine) and the elevation of lipid biomarkers (palmitoyl sphingomyelin and phosphatidylcholine). These changes may serve as early indicators of THS-induced toxicity, offering a window for preventive intervention before the onset of haematological and pulmonary impairments. Moreover, the association between metabolic alterations and inflammatory processes, particularly pyroptosis as indicated by IL-18, provides mechanistic insights into THS-induced pyroptosis and cellular dysfunction. This study is among the 1st to explore the utility of chromatographic profiling in THS research, highlighting its capacity to reveal subtle metabolic shifts that conventional toxicological assessments may overlook. By establishing a link between metabolic disturbances and inflammatory responses, it contributes to a deeper understanding of the systemic effects of THS exposure. These findings lay the groundwork for further investigations into the early biomarkers of THS-related health risks.

Nevertheless, the study has certain limitations. The sample size, while sufficient for preliminary observations, warrants expansion in future research to enhance statistical robustness. However, as an exploratory investigation, this study shares characteristics with pilot studies [39]. While the sample size is relatively modest, this study was designed as an exploratory toxicological investigation aimed at identifying early metabolic disruptions rather than establishing definitive dose-response relationships or population-wide effects. Previous research (not a pilot study) has also employed 4 - 6 rats per group in toxicological studies involving tobacco smoke exposure [40], supporting the feasibility of our approach. We performed calculations using OpenEpi, as recommended by [39]. Another study [41] which included n = 6 per group, served as a reference for our sample size estimation, employing "mean difference" panel with data from that study for the mean and standard deviation benchmark, a 95 % confidence interval, and 80 % power. The results indicated that a sample size of 5 rats per group exceeded the recommended threshold. This study adheres to the 3Rs principle (Replacement, Reduction, and Refinement), advocating for the ethical use of animals in research while ensuring scientific rigour.

Another limitation is this study did not include a full validation of the LC-MS method with respect to precision, linearity, and detection limits, as its primary objective was to explore metabolic alterations associated with THS exposure rather than to develop a fully validated analytical method to quantify specific

target (absence of predefined target compounds). However, we ensured consistent instrument performance by adhering to standard LC-MS protocols.

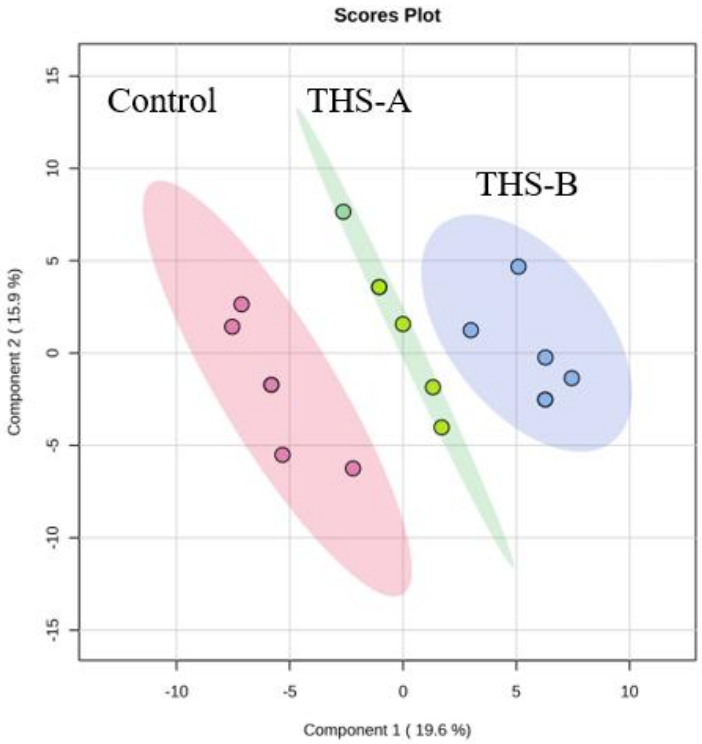

Figure 6 The PLS-DA score plot illustrating the metabolic profile differentiation among the 3 experimental groups: Control (pink), THS-A (green), and THS-B (blue). Each point represents an individual sample. The separation observed suggests distinct metabolic variations between the groups.

Furthermore, PLS-DA analysis was performed using the MetaboAnalyst web-based platform, demonstrating clear separation between the experimental groups (**Figure 6**). To enhance the reliability of our findings, we repeated the PLS-DA analysis multiple times and consistently obtained similar clustering patterns, reinforcing the robustness of our observations. Although additional validation procedures such as permutation testing and the reporting of R^2 and Q^2 values—would further enhance the robustness of the model, the observed clustering, together with the statistically significant ANOVA result for phosphatidylcholine in particular (p = 0.0002156), suggests biologically meaningful metabolic differences between the groups.

Further studies incorporating larger sample sizes, thorough validation of the LC-MS methodology, and more rigorous evaluation of multivariate models are recommended to verify and extend the metabolic alterations identified in this exploratory study.

Conclusions

This study highlights the potential of chromatography as a sensitive and reliable tool for the early detection of metabolic disturbances in amino acid and lipid homeostasis, serving as preclinical biomarkers of THS-induced toxicity. Unlike routine haematological assessments, which primarily detect systemic changes at later stages, chromatographic profiling enables the identification of subtle biochemical alterations at an earlier phase. The detection of key amino acid depletions and change in lipid homeostasis as early as day 10 underscores its capacity to reveal underlying metabolic imbalances before conventional markers indicate pathological changes. By integrating chromatography-based techniques into environmental and occupational health monitoring, this approach

provides a more comprehensive method for assessing hidden toxicant exposure and its potential long-term effects. Given the growing concern over THS exposure, these findings underscore the necessity of adopting advanced analytical methodologies for early toxicological assessment. Future studies involving larger cohorts and human biomonitoring will be essential to further validate the applicability of this approach in real-world exposure scenarios.

Acknowledgements

To Mr. Suratno for his support in chromatography, Assoc-Professor Nur Arfian, Tiara Kurniasari, Ando Gavintri, and Safira for technical expertise in animal treatments. To Fatin Asfarina, for molecular laboratory assistance.

References

[1] P Jacob, NL Benowitz, H Destaillats, L Gundel, B Hang, M Martins-Green, GE Matt, PJE Quintana, JM Samet, SF Schick, P Talbot, N Aquilina, MF Hovell, JH Mao and TP Whitehead. Thirdhand smoke: New evidence, challenges, and future directions. *Chemical Research in Toxicology* 2017; **30(1)**, 270-294.

[2] B Hang, AH Sarker, C Havel, S Saha, TK Hazra, S Schick, P Jacob, VK Rehan, A Chenna, D Sharan, M Sleiman, H Destaillats and LA Gundel. Thirdhand smoke causes DNA damage in human cells. *Mutagenesis* 2013; **28(4)**, 381-391.

[3] M Martins-Green, N Adhami, M Frankos, M Valdez, B Goodwin, J Lyubovitsky, S Dhall, M Garcia, I Egiebor, B Martinez, HW Green, C Havel, L Yu, S Liles, G Matt, H Destaillats, M Sleiman, LA Gundel, N Benowitz, P Jacob, M Hovell, JP Winickoff and M Curras-Collazo. Cigarette smoke toxins deposited on surfaces: Implications for human health. *PLoS One* 2014; **9(1)**, e86391.

[4] National Center for Biotechnology Information, Methanol. PubChem Compound Summary, Available at: https://pubchem.ncbi.nlm.nih.gov/compound/Methanol, Accessed March 2025.

[5] M Fischer and TM Jefferies. Optimization of nicotine extraction from tobacco using supercritical fluid technology with dynamic extraction modeling. *Journal of Agricultural and Food Chemistry* 1996; **44(5)**, 1258-1264.

[6] H Nerome, M Ito, S Machmudah, Wahyudiono, H Kanda and M Goto. Extraction of phytochemicals from saffron by supercritical carbon dioxide with water and methanol as entrainer. *Journal of Supercritical Fluids* 2016; **107**, 377-383.

[7] B Hang, AM Snijders, Y Huang, SF Schick, P Wang, Y Xia, C Havel, P Jacob, N Benowitz, H Destaillats, LA Gundel and JH Mao. Early exposure to third-hand cigarette smoke affects body mass and the development of immunity in mice. *Scientific Reports* 2017; **7**, 41915.

[8] A Windarsih, FDO Riswanto, NKA Bakar, ND Yuliana, Dachriyanus and A Rohman. Detection of pork in beef meatballs using LC-HRMS based untargeted metabolomics and chemometrics for halal authentication. *Molecules* 2022; **27(23)**, 8325.

[9] TV Hoang, C Nardiello, DES Solaligue, JA Rodríguez-Castillo, P Rath, K Mayer, I Vadász, S Herold, K Ahlbrecht, W Seeger and RE Morty. Stereological analysis of individual lung lobes during normal and aberrant mouse lung alveolarisation. *Journal of Anatomy* 2018; **232(3)**, 472-484.

[10] YH Chung, M Gulumian, RC Pleus and IJ Yu. Animal welfare considerations when conducting OECD test guideline inhalation and toxicokinetic studies for nanomaterials. *Animals* 2022; **12(23)**, 3305.

[11] GE Matt, PJE Quintana and H Destaillats. Third-hand smoke: Chemical dynamics, exposure, and health effects. *Environmental Research* 2018. https://doi.org/10.3390/atmos16040370

[12] JR Smith, ER Bolton and MR Dwinell. The rat: A model used in biomedical research. *Methods in Molecular Biology* 2019; **2018**, 1-41.

[13] EM Blais, KD Rawls, BV Dougherty, ZI Li, GL Kolling, P Ye, A Wallqvist and JA Papin. Reconciled rat and human metabolic networks for comparative toxicogenomics and biomarker predictions. *Nature Communications* 2017; **8**, 14250.

[14] D Villalobos-García, HEA Ali, AB Alarabi, MS El-Halawany, FZ Alshbool and FT Khasawneh. Exposure of mice to third-hand smoke modulates

in vitro and *in vivo* platelet responses. *International Journal of Molecular Sciences* 2022; **23(10)**, 5595.

[15] J Ho, K Koshibu, W Xia, K Luettich, A Kondylis, L Garcia, B Phillips, M Peitsch and J Hoeng. Effects of cigarette smoke exposure on a mouse model of multiple sclerosis. *Toxicology Reports* 2022; **9**, 597-610.

[16] M Sleiman, LA Gundel, JF Pankow, P Jacob, BC Singer and H Destaillats. Formation of carcinogens indoors by surface-mediated reactions of nicotine with nitrous acid, leading to potential third-hand smoke hazards. *Proceedings of the National Academy of Sciences of the United States of America* 2010; **107(15)**, 6576-6581.

[17] SF Schick and SA Glantz. Thirdhand smoke: Here to stay. *Tobacco Control* 2011; **20(1)**, 1-3.

[18] S Torres, C Merino, B Paton, X Correig and N Ramírez. Biomarkers of exposure to secondhand and thirdhand tobacco smoke: Recent advances and future perspectives. *International Journal of Environmental Research and Public Health* 2018; **15(12)**, 2693.

[19] Y Tateishi, S Toyoda, H Murakami, R Uchida, R Ichikawa, T Kikuchi, W Sato and K Suzuki. A short-term intervention of ingesting iron along with methionine and threonine leads to a higher hemoglobin level than that with iron alone in young healthy women: A randomized, double-blind, parallel-group, comparative study. *European Journal of Nutrition* 2023; **62(7)**, 3009-3019.

[20] JK Lugata, J Oláh, XE Ozsváth, R Knop, E Angyal and C Szabó. Effects of DL and L-methionine on growth rate, feather growth, and hematological parameters of tetra-SL layers from 1-28 days of age. *Animals* 2022; **12(15)**, 1928.

[21] A Vlachos, E Atsidaftos, ML Lababidi, E Muir, ZR Rogers, W Alhushki, J Bernstein, B Glader, B Gruner, H Hartung, C Knoll, T Loew, G Nalepa, A Narla, AR Panigrahi, CA Sieff, K Walkovich, JE Farrar and JM Lipton. L-leucine improves anemia and growth in patients with transfusion-dependent Diamond Blackfan anemia: Results from a multicenter pilot phase I/II study from the Diamond Blackfan Anemia Registry. *Pediatric Blood and Cancer* 2020; **67(12)**, e28748.

[22] M Malaguarnera, M Vacante, M Giordano, M Motta, G Bertino, M Pennisi, S Neri, M Malaguarnera, GL Volti and F Galvano. L-carnitine supplementation improves hematological pattern in patients affected by HCV treated with Peg interferon-α 2b plus ribavirin. *World Journal of Gastroenterology* 2011; **17(39)**, 4414-4420.

[23] YA Hannun and LM Obeid. Sphingolipids and their metabolism in physiology and disease. *Nature Reviews Molecular Cell Biology* 2018; **19**, 175-191.

[24] X Rao, D Zhou, H Deng, Y Chen, J Wang, X Zhou, X Jie, Y Xu, Z Wu, G Wang, X Dong, S Zhang, R Meng, C Wu, S Xing, K Fan, G Wu and R Zhou. Activation of NLRP3 inflammasome in lung epithelial cells triggers radiation-induced lung injury. *Respiratory Research* 2023; **24(1)**, 25.

[25] EH Koh, JE Yoon, MS Ko, J Leem, JY Yun, CH Hong, YK Cho, SE Lee, JE Jang, JY Baek, HJ Yoo, SJ Kim, CO Sung, JS Lim, WI Jeong, SH Back, IJ Baek, S Torres, E Solsona-Vilarrasa, LCDL Rosa, C Garcia-Ruiz, AE Feldstein, JC Fernandez-Checa and KU Lee. Sphingomyelin synthase 1 mediates hepatocyte pyroptosis to trigger non-alcoholic steatohepatitis. *Gut* 2021; **70(10)**, 1954-1964.

[26] F Liu, Y Zhang, Y Shi, K Xiong, F Wang and J Yang. Ceramide induces pyroptosis through TXNIP/NLRP3/GSDMD pathway in HUVECs. *BMC Molecular and Cell Biology* 2022; **23**, 54.

[27] JNVD Veen, JP Kennelly, S Wan, JE Vance, DE Vance and RL Jacobs. The critical role of phosphatidylcholine and phosphatidylethanolamine metabolism in health and disease. *Biochimica et Biophysica Acta - Biomembranes* 2017; **1859(9)**, 1558-1572.

[28] A Javdani-Mallak and I Salahshoori. Environmental pollutants and exosomes: A new paradigm in environmental health and disease. *Science of the Total Environment* 2024; **925**, 171774.

[29] K Weigand, G Peschel, J Grimm, M Höring, S Krautbauer, G Liebisch, M Müller and C Buechler. Serum phosphatidylcholine species 32:0 as a biomarker for liver cirrhosis pre- and post-

hepatitis C virus clearance. *International Journal of Molecular Sciences* 2024; **25(15)**, 8161.

[30] R Muraki, Y Morita, S Ida, R Kitajima, S Furuhashi, M Takeda, H Kikuchi, Y Hiramatsu, Y Takanashi, Y Hamaya, K Sugimoto, J Ito, K Kawata, H Kawasaki, T Sato, T Kahyo, M Setou and H Takeuchi. Phosphatidylcholine in bile-derived small extracellular vesicles as a novel biomarker of cholangiocarcinoma. *Cancer Medicine* 2023; **12(12)**, 13007-13018.

[31] K Muta, K Saito, Y Kemmochi, T Masuyama, A Kobayashi, Y Saito and S Sugai. Phosphatidylcholine (18:0/20:4), a potential biomarker to predict ethionamide-induced hepatic steatosis in rats. *Journal of Applied Toxicology* 2022; **42(9)**, 1533-1547.

[32] SH Yeon, G Yang, HE Lee and JY Lee. Oxidized phosphatidylcholine induces the activation of NLRP3 inflammasome in macrophages. *Journal of Leukocyte Biology* 2017; **101(1)**, 205-215.

[33] E Vianello, F Ambrogi, M Kalousová, J Badalyan, E Dozio, L Tacchini, G Schmitz, T Zima, GJ Tsongalis and MM Corsi-Romanelli. Circulating perturbation of phosphatidylcholine (PC) and phosphatidylethanolamine (PE) is associated to cardiac remodeling and NLRP3 inflammasome in cardiovascular patients with insulin resistance risk. *Experimental and Molecular Pathology* 2024; **137**, 104895.

[34] R Corrêa, LFF Silva, DJS Ribeiro, RDN Almeida, IDO Santos, LH Corrêa, LPD Sant'Ana, LS Assunção, PT Bozza and KG Magalhães. Lysophosphatidylcholine induces NLRP3 inflammasome-mediated foam cell formation and pyroptosis in human monocytes and endothelial cells. *Frontiers in Immunology* 2020; **10**, 2927.

[35] L Zhang, R Lukowski, F Gaertner, M Lorenz, KR Legate, K Domes and S Offermanns. Thrombocytosis as a response to high interleukin-6 levels in cGMP-dependent protein kinase I mutant mice. *Arteriosclerosis, Thrombosis, and Vascular Biology* 2013; **33(8)**, 1820-1828.

[36] A Kaser, G Brandacher, W Steurer, S Kaser, FA Offner, H Zoller, I Theurl, W Widder, C Molnar, O Ludwiczek, MB Atkins, JW Mier and H Tilg. Interleukin-6 stimulates thrombopoiesis through thrombopoietin: Role in inflammatory thrombocytosis. *Blood* 2001; **98(9)**, 2720-2725.

[37] T Ganz. Anaemia of inflammation. *New England Journal of Medicine* 2019; **381(12)**, 1149-1157.

[38] L Lanser, D Fuchs, K Kurz and G Weiss. Physiology and inflammation-driven pathophysiology of iron homeostasis - Mechanistic insights into anaemia of inflammation and its treatment. *Nutrients* 2021; **13(11)**, 3732.

[39] COS Sorzano, D Tabas-Madrid, F Núñez, C Fernández-Criado and A Naranjo. Sample size for pilot studies and precision-driven experiments. *arXiv* 2017. https://doi.org/10.48550/arXiv.1707.00222

[40] AK Pham, CW Wu, X Qiu, J Xu, S Smiley-Jewell, D Uyeminami, P Upadhyay, D Zhao and KE Pinkerton. Differential lung inflammation and injury with tobacco smoke exposure in Wistar Kyoto and spontaneously hypertensive rats. *Inhalation Toxicology* 2020; **32(8)**, 328-341.

[41] F Vivarelli, C Morosini, L Rullo, LM Losapio, A Lacorte, S Sangiorgi, S Ghini, I Fagiolino, P Franchi, M Lucarini, S Candeletti, D Canistro, P Romualdi and M Paolini. Effects of unburned tobacco smoke on inflammatory and oxidative mediators in the rat prefrontal cortex. *Frontiers in Pharmacology* 2024; **15**, 1328917.